2018 European Control Conference (ECC)
June 12-15, 2018. Limassol, Cyprus

Mild-Hybrid Electric Vehicle: EM management to prevent dry clutch overheating

Mario Pisaturo, Adolfo Senatore

Abstract— **Heat power generated in dry clutch systems during repeated engagements could result in marked uncomfort and manifest damage clutch facing materials. Indeed, recent studies have highlighted as during a single launch manoeuvre the interface temperature can amount about 30-35 Celsius degree. Consequently, after only few repeated engagements in short time the clutch material temperature can attain critical values, i.e. 250-300 Celsius degree. For this reason, the electric motor contribution to reduce overheating of clutch material during the slipping phase could represent a good solution to avoid dry clutch damage. In this paper a high-level Model Predictive Controller with time-variant penalty weights accordingly with working conditions has been implemented. The goal of this study is to manage both internal combustion engine and electric motor during clutch engagements in order to relieve dry clutch during a critical launch manoeuvre. Particularly, the following scenario has been assumed: high initial clutch temperature due to previous repeated engagements, up-hill start-up manoeuvre and low initial SOC.**

I. INTRODUCTION

Hybrid Electric Vehicles (HEVs) was introduced to combine the advantages of internal combustion engine (ICE) in terms of covered mileage and electric motor (EM) in terms of energy efficiency and low pollutant emissions. To this aim, several architectures have been proposed: parallel, series, series-parallel and complex. In parallel HEVs both the ICE and EM can propel, separately or at same time, the wheels. This solution conceptually can be seen as electric-assisted ICE vehicle for achieving both lower emissions and fuel consumption [1]. On the other hand, in series HEVs the ICE output is converted into electric energy in order to charge the battery pack or to propel the wheels. Thus, this system needs three devices: the ICE, the generator and the electric motor, to propel the wheels. The main disadvantages of series HEVs are low efficiency and high costs because all the devices need to be sized for the maximum sustained power. Finally, in the series-parallel configuration the features of both the series and parallel HEVs are incorporated but to the detriment of simplicity and costs. Finally, all configurations that cannot be classified in the three typologies seen before are called complex HEVs [1]. The cost production both of full electric and full hybrid vehicles is probably the main reason of their poor diffusion. Thus, in these years low hybridization level solutions have been proposed to limit costs and improving fuel economy. The first level is the so-called idle stop-start feature which allows to reduce the fuel consumption of about $3-10\%$ [2]. In this case the typical alternator is replaced with an integrated starter generator (ISG). To introduce more features as the ability to start the engine, provide electric assist, maintain regenerative braking, and serve as a generator a higher hybridization level was proposed. This solution is called mild-HEV and the power range of the ISG is $7-15$ kW. A simple and inexpensive solution is mounting the ISG in the conventional location of the starter motor or generator to couple with the flywheel and engine via the belt, it is so-called the belt-driven ISG also called belt starter generator (BSG). Another solution is to directly mounting the ISG onto the crankshaft, in this case the ISG rotor can serve as the flywheel inertia so that the aforementioned flywheel coupled with the engine can be eliminated [3]. Mild-HEVs allow to reduce the fuel consumption of about $10-16\%$ [2].

In these years numerous control strategies have been proposed for HEVs both to optimize the transition between the two propulsion devices in order to improve comfort [4]–[6] and to minimizes the fuel consumption over a given driving schedule [7]–[9] keeping the balance of battery state of charge (SOC) [10]–[12].

In this study the influence of EM in parallel mild-HEVs is analysed in order to investigate its possible helpful role to reduce the temperature rise in dry clutch Automated Manual Transmission (AMT) during the slipping phase. In fact, one of the most important issue in dry clutch architectures like AMTs and Dual Clutch Transmissions (DCT) is the overheating due to repeated engagements [13]–[15] which results in poor engagements (engine switching off, torque fluctuations and poor comfort perceived by car passengers) or even detriment of clutch linings [16], [17]. Thus, to avoid to attain critical values and improve passengers comfort, the role of the EM to relieve heat generation in dry clutch system has been investigate. A Model Predictive Control (MPC) with time-variant penalty weights has been designed to manage both ICE and EM by taking also into account the battery SOC. Particularly, the following scenario has been assumed: high initial clutch temperature due to previous repeated engagements, up-hill start-up manoeuvre and a given initial SOC. Finally, the simulation results have underlined that the EM contribute can effectively reduce the thermal field during the slipping phase without significantly decrease the SOC.

II. PARALLEL HEV

A. Driveline model

In this section the driveline model used for simulating the parallel mild-HEV longitudinal dynamics is presented Fig. 1. Where T indicates the torques, J the inertias and b the

*This work was not supported by any organization

Mario Pisaturo and Adolfo Senatore are with Department of Industrial Engineering, University of Salerno, 84084 Fisciano SA, Italy mpisaturo@unisa.it, a.senatore@unisa.it

damping coefficients. Whereas, the subscripts *e*, *f*, *c*, *g*, *d*, *m*, *w* indicate engine, flywheel, clutch disc, gearbox, differential, electric motor and wheels, respectively. In typical configurations the starter generator is mounted before the clutch. Conversely, in the proposed configuration the electric motor is mounted after the clutch in order to relieve it from thermal stress in heavy start up manoeuvres. Indeed, only in this way it is possible to deliver torque to the wheels bypassing the clutch. Under the hypothesis that all shafts are rigid, the synchronizer dynamics can be neglected as well as gears are ideal, i.e. $\omega_w = \frac{\omega_c}{r_1 r_d} = \frac{\omega_m}{r_2 r_d}$ the following equations hold:

$$J_{ef}\dot{\omega}_e = T_e - b_e\omega_e - T_{fc} \tag{1}$$

$$J_v\dot{\omega}_w = r_1 r_d T_{fc} + s r_2 r_d T_m + \\ - \left(b_g \left(r_1 r_d\right)^2 + s b_m \left(r_2 r_d\right)^2\right)\omega_w - T_w \tag{2}$$

where r_1, r_2 and r_d are the gear ratios on the engine side, electric motor side and differential respectively. Moreover, s is a parameter equal to 1 when the electric motor is active (HEV mode) and 0 when it is inactive (ICE only mode). In addition, the following positions hold:

$$J_{ef} = J_e + J_f \tag{3}$$

$$J_v = J_w + J_d + \left(J_{g2}\right) r_d^2 + \left(J_{g1} + J_c\right)\left(r_1 r_d\right)^2 + \\ + \left(J_{g3} + s J_m\right)\left(r_2 r_d\right)^2 \tag{4}$$

$$T_w = mgR_w\left(\sin(\phi) + f\cos(\phi)\right) + \\ + \frac{1}{2}\rho_{aria} A C_x v^2 R_w + T_{brake} \tag{5}$$

where, m is the vehicle mass, R_w is the wheel radius, ϕ is the road slope, f is the rolling resistance coefficient, ρ_{aria} is the air density, A is the vehicle frontal area, C_x is the air drag coefficient, v the vehicle speed and T_{brake} is the braking torque. The equation which represents the "locked-up" model can be derived from (1) and (2) by taking into account driveline dynamics reduced to engine (or wheel) side. A state-space representation has been used to design the MPC [18], [19].

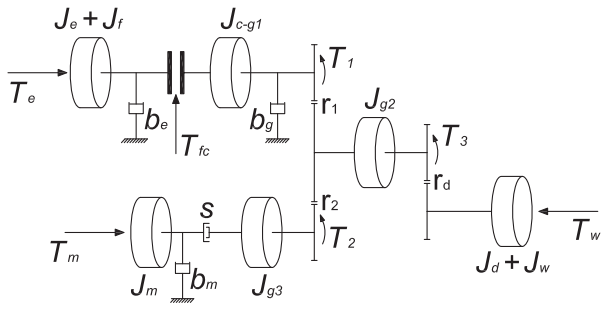

Fig. 1. Driveline model

B. ICE model

To simulate the engine behaviour an engine static map has been implemented in the Simulink model. In particular, the inputs of the static map are the engine angular speed ("plant" output) and the accelerator pedal signal. This latter is obtained by means an inverted engine map which is fed by the reference engine torque (first MPC output). More details on the engine model can be found in [20].

III. CLUTCH MODEL

The torque transmitted by a dry clutch is mainly affected by the friction coefficient and the cushion spring characteristic [21]. In particular, the friction phenomena between friction pads on the two sides of the clutch disk and flywheel on one side and pressure plate on the other side result in a temperature rise which influences both the friction coefficient [17], [22]–[25] and cushion spring [26]–[28] behaviours. To take into account these thermal effects a complex transmissibility model has been proposed in [22] and reported in (6).

$$T_{fc}(x_{to}, \theta_{cs}, \theta_{cm}, v_s, p) = \\ = n\mu(v_s, p, \theta_{cm}) R_m F_{fc}(\delta_f(x_{pp}(x_{to}, \theta_{cs}), \theta_{cs})) \tag{6}$$

where the clutch torque T_{fc} has been assumed proportional to the cushion spring load-deflection characteristic F_{fc} through the friction coefficient map $\mu(v_s, p, \theta_{cm})$, the number of friction surfaces n and the geometrical parameter R_m. Moreover, the electro-hydraulic actuator dynamics has been simulated by implementing a unitary gain first-order transfer function with time constant equal to 0.1 s. For the sake of brevity, details on the transmissibility model are omitted but the Reader can find them in the cited literature. Finally, the reference clutch torque (second MPC output) is inverted by means of a simplified clutch model to get the reference throwout bearing position. This signal, coupled to actuator dynamics, has been used as input in a detailed clutch torque map (n-D look-up table) [23] to obtain the actual clutch torque ("plant" input).

A. Thermal model

In order to implement the clutch transmissibility model described in (6) it is necessary to calculate both the clutch material and the cushion spring temperatures. To this aim a lumped thermal model has been introduced to estimate the average temperature on the clutch facing and on the cushion spring during the slipping phase [14], [29]. The first assumption is that the whole mechanical work is converted into heat by friction phenomena and it is equally distributed onto the friction surfaces. Moreover, when the clutch is open, i.e. $\beta = 0$, only convective losses take place whereas when the clutch is in the slipping phase, i.e. $\beta = 1$, only conductive phenomena occur and the convective losses are negligible on cushion spring and clutch material. On the contrary, the body convective losses cannot be neglected when the clutch is closed. For this reason, the term $(2 - \beta)$ accounts for about doubled clutch surface active to convective heat exchange when the clutch is open. Thus, the thermal dynamics of clutch material θ_{cm}, body θ_b and cushion spring θ_{fs} is

provided by first order differential equations:

$$\begin{cases} \dot{\theta}_b = \alpha_1\beta\left(\theta_{cm}-\theta_b\right)-\alpha_2\left(2-\beta\right)\left(\theta_b-\theta_h\right)+ \\ +\alpha_3\frac{T_{fc}\omega_{sl}}{2} \\ \dot{\theta}_{cm} = -\alpha_4\beta\left(\theta_{cm}-\theta_b\right)+ \\ -\alpha_5\left(1-\beta\right)\left(\theta_{cm}-\theta_h\right)-\alpha_6\left(\theta_{cm}-\theta_{fs}\right)+ \\ +\alpha_7\frac{T_{fc}\omega_{sl}}{2} \\ \dot{\theta}_{fs} = 2\alpha_8\left(\theta_{cm}-\theta_{fs}\right)-\alpha_9\left(1-\beta\right)\left(\theta_{cm}-\theta_h\right) \end{cases} \tag{7}$$

where θ_h is the ambient temperature assumed constant and α_i are the thermal parameters identified by means the FE results reported in [13] by considering the same thermal power as input.

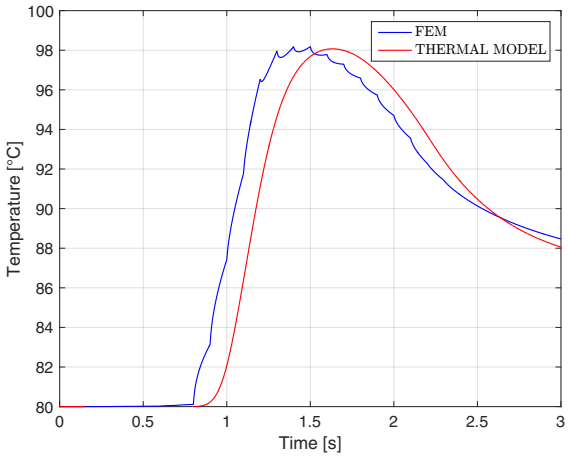

Fig. 2. Comparison between FEM [13] and lumped thermal model

IV. ELECTRIC MOTOR AND ENERGY STORAGE MODELS

A. PMSM model

The dynamics of a Permanent Magnet Synchronous Machine (PMSM) is described in this section. The fast torque responses coupled to its high performances makes it a good solution for automotive applications. A PMSM has a stator with three windings (one per phase) whereas permanent magnets are mounted on (or inside) the rotor [30]. The first one is called Surface Mounted PMSM and the second one Interior PMSM. To reduce the mathematical model complexity the Surface Mounted PMSM dynamics is usually written in the rotor $d-q$ reference frame [31]. The voltage equations are:

$$\begin{cases} v_{sd} = R_s i_{sd} + L_s\frac{di_{sd}}{dt} - \omega L_s i_{sq} \\ v_{sq} = R_s i_{sq} + L_s\frac{di_{sq}}{dt} - \omega\left(L_s i_{sd}+\Phi\right) \end{cases} \tag{8}$$

where i_{sd} and i_{sq} are the stator currents in the d and q direction, R_s and L_s are the stator phase resistance and inductance respectively ω is the electrical speed, v_{sd} and v_{sq} are the stator voltages reported in the $d-q$ system of coordinates and Φ is the rotor permanent magnet flux. It is worth noting that the electrical angular speed is: $\omega = N\omega_m$ where N is the number of pole pairs and ω_m is the mechanical angular speed which depends from the driveline dynamics. R_s, L_s and Φ are considered as constants. These equations are used to implement PI control strategies for a direct electric motor torque control. As mentioned before, a hierarchical approach is used, in fact the MPC gives as third output the reference electric motor torque whereas the PI regulators deliver signals to the inverter in order to manage the PMSM dynamics. The inverter dynamics has been assumed as a first order transfer function according to [32]. The electric motor efficiency has been taken into account by using a static map. Furthermore, since the start-up manoeuvre has a short duration the electric motor thermal dynamics has been neglected. Finally, the power split mode, i.e. ICE power is split to drive the vehicle and charge the battery (motor becomes generator), the stationary charging mode and the regenerative braking mode are not considered in the purpose of this paper.

B. Battery model

To calculate the SOC evolution during the engagement manoeuvre a battery model has been implemented. Both the open circuit voltage V_{oc} and the equivalent internal resistance R_{int} have been considered dependent from SOC level and temperature by using look-up tables. The battery thermal dynamics has been neglected as the short duration of the start-up manoeuvre, thus a constant temperature has been assumed. The battery current is calculated as follows:

$$I_{batt} = \frac{V_{oc}-\sqrt{V_{oc}^2-4R_{int}P_{req}}}{2R_{int}} \tag{9}$$

where the required power has been estimated as $P_{req} = \frac{T_m\omega_m}{\eta_m}$ with η_m obtained from the electric motor efficiency map. Finally, the SOC is obtained by the following equation:

$$SOC = SOC_0 - \frac{\int_{t_1}^{t_2} I_{batt}\left(t\right)dt}{Q_{max}} \tag{10}$$

where SOC_0 is the initial SOC, Q_{max} is the max battery capacity equal to $2.5\ Ah$ and the integral in numerator is the used capacity during the discharge phase [33], [34]:

V. MODEL PREDICTIVE CONTROL DESIGN

The model predictive control has been designed with the discrete time version of the state space representation of the driveline (1) and (2). It has been used the zero-order hold method with a sampling time of $0.01\ s$. In fact, as reported in [35] the computational cycle adopted for these applications is set as 5 to 10 ms. As well known, the clutch could have two main phases: slipping and engaged. Particularly, the engaged condition is attained when the slip speed $\omega_{sl} = |\omega_e - \omega_c| \leq 1\ rad/s$. Moreover, due to discrete domain of the variable s, the "plant" dynamics is switching. The controller has been designed by considering only the slipping phase and the switching variable $s = 1$, i.e. parallel HEV mode. Thus, a deep analysis on the stability of the "plant" dynamics with the changing s has not been performed in this paper. The

state-space representation used to design the MPC is reported below:

$$\begin{cases} \mathbf{x}_{k+1} = \bar{\mathbf{A}}\mathbf{x}_k + \bar{\mathbf{B}}\mathbf{u}_k \\ \mathbf{y}_k = \bar{\mathbf{C}}\mathbf{x}_k \end{cases} \tag{11}$$

where $\mathbf{x} = [\omega_e\ \omega_w]^T$ is the state vector, $\mathbf{y} = [\omega_e\ \omega_c]^T$ is the output vector and $\mathbf{u} = [T_e\ T_{fc}\ T_m\ T_w]^T$ is the input vector. To design the controller it has been assumed that ω_e and ω_w are measured output. Moreover, T_e, T_{fc} and T_m are manipulated variables whereas T_w is a measured disturbance [36], [37]. The MPC has the role of high-level controller which generates reference signals to low-level PI regulators according to actuators constraints and "plant" working conditions. Moreover, a control strategy which has time-variant penalty weights has been implemented to trigger the electric motor on if clutch material is undergone to high thermal stress.

A. Plant constraints

As mentioned before, to take into account actuators limitations some constraints on the "plant" input have been implemented in the MPC .

$$-73 \leq T_e \leq 320 \quad Nm \tag{12}$$

$$\dot{T_e} \leq 200 \quad Nm/s \tag{13}$$

$$0 \leq T_{fc} \leq 425 \quad Nm \tag{14}$$

$$0 \leq T_m \leq 140 \quad Nm \tag{15}$$

Minimum motor torque has been set to zero as the regenerative phase has not been simulated in this paper.

Besides, to avoid the engine stall condition and guarantee comfortable lock-up some constraints have been adopted also on the "plant" outputs, i.e. engine and clutch angular speeds.

$$60 \leq \omega_e \leq 600 \quad rad/s \tag{16}$$

$$\omega_c \geq 0 \quad rad/s \tag{17}$$

B. Optimization problem and tuning

As previously explained, time-variant penalty weights have been implemented to prevent clutch overheating by reducing the thermal power dissipated during the slipping phase. Particularly, if the estimated clutch material temperature reaches or overcomes the trigger temperature of $200\,^{\circ}\mathrm{C}$ the EM penalization is switched to zero. On the contrary, when the estimated temperature is below the threshold temperature, the EM penalization weight is high in order to inhibit the EM activation. The cost function to be minimized, by satisfying constraints each time step, is reported in (18).

$$\begin{aligned} J = &[\mathbf{y}_j - \mathbf{r}_j]^T \mathbf{W}_{y,j}^2 [\mathbf{y}_j - \mathbf{r}_j] + ... \\ &+[\mathbf{u}_i - \mathbf{u}_{\mathrm{target},i}]^T \mathbf{W}_{u,i}^2 [\mathbf{u}_i - \mathbf{u}_{\mathrm{target},i}] + ... \\ &+\Delta\mathbf{u}_i^T \mathbf{W}_{\Delta u,i}^2 \Delta\mathbf{u}_i + \rho_\varepsilon \varepsilon^2 \end{aligned} \tag{18}$$

where: $\mathbf{u}_i = \begin{bmatrix} u_i(0) & ... & u_i(P-1) \end{bmatrix}^T$ is the input vector;

$\mathbf{u}_{\mathrm{target},i} = \begin{bmatrix} u_{\mathrm{target,i}}(0) & ... & u_{\mathrm{target,i}}(P-1) \end{bmatrix}^T$ is the input target vector; $\Delta\mathbf{u}_i = \begin{bmatrix} \Delta u_i(0) & ... & \Delta u_i(P-1) \end{bmatrix}^T$ is the input increment vector;

$\mathbf{y}_j = \begin{bmatrix} y_j(1) & ... & y_j(P) \end{bmatrix}^T$ is the output vector;

$\mathbf{r}_j = \begin{bmatrix} r_j(1) & ... & r_j(P) \end{bmatrix}^T$ is the reference trajectory vector;

$\mathbf{W}_{u,i}$, $\mathbf{W}_{\Delta u,i}$ and $\mathbf{W}_{y,j}$ are, respectively, the input, input increment and output scaled weights matrices (diagonals and squares). Finally, the subscript i and j take into account the ith inputs and jth outputs of the "plant" respectively. The constraints on $\mathbf{u}$, $\Delta\mathbf{u}$, and $\mathbf{y}$ are softened by introducing the dimensionless non-negative slack variable ε. The controller aims at keeping plant outputs as close as possible to the reference signals. Also the manipulated variables, i.e. plant inputs, must be the closest possible their target values by avoiding large fluctuations in one step. For this reason a tuning procedure of some controller parameters is necessary. The parameters to be tuned are the prediction horizon P, the control horizon m, the input, input increments and output scaled weights matrices $W_{u,i}$, $W_{\Delta u,i}$, $W_{y,j}$ respectively, and overall penalty weight ρ_ϵ.

C. Temperature estimation

As explained before, the electric motor activation is requested only if the clutch material temperature tends to a critical value, assumed to be $250\,^{\circ}\mathrm{C}$. For this reason, a safety threshold temperature of $200\,^{\circ}\mathrm{C}$ has been implemented in the control strategy to trigger the hybrid mode on and reduce the thermal power generated during the sliding phase, and consequently the temperature rise. Unfortunately, no direct measure of the interface temperature is available in real system; so dedicated algorithms are used to capture the clutch thermal dynamics [14], [38], [39]. Thus, to estimate the clutch material temperature the system (7) has been adopted in the transmission control unit. It is worth noting that it is necessary to know the ambient temperature θ_h and the thermal power, given by the product between the clutch torque T_{fc} and the sliding speed ω_{sl}. About the ambient temperature, it can be directly measured or assumed equal to engine induct air temperature [38]. Instead, the sliding speed $\omega_{sl} = |\omega_e - \omega_c|$ is considered known at each time step as the engine speed ω_e is directly measured whereas the clutch angular speed can be estimated from wheel angular speed, which is directly measured also, by assuming all shafts rigid $\omega_c = r_1 r_d \omega_w$. The only unknown variable is the transmitted clutch torque which is not measured. Different methods can be used to estimate it in real-time [40]–[42]. In this paper, the reference clutch torque output of the MPC has been used for temperature estimation purpose.

VI. SIMULATION RESULTS

The simulations results have been obtained by taking into account the following scenario: high initial clutch temperature (i.e. $190\,^{\circ}\mathrm{C}$) due to previous repeated engagements, up-hill start-up (road slope of 5 degree) and an initial SOC of 0.25. Under these hypotheses the role of the electric motor has been investigated to reduce contact surfaces overheating

without significantly decrease the SOC. To this aim a custom Matlab/Simulink model which takes into account both a detailed dry clutch torque transmissibility model (i.e. by considering cushion spring thermal expansion and temperature-pressure-sliding speed dependent friction coefficient) and electric motor dynamics has been taken into account to simulate the longitudinal vehicle dynamics.

As explained in the previous section, time-variant penalty weights according to working conditions have been considered in the control strategy. The electric motor is triggered on if the estimated temperature is higher than the activation temperature threshold of $200\,^{\circ}\mathrm{C}$. In Figs. 3, 4 and 5 the results of the analysed launch manoeuvre both for the hybrid and ICE only mode are reported. In Fig. 3 is shown how in the HEV mode the clutch angular speed, i.e. the vehicle acceleration, is higher than the ICE only mode. In fact, in the hybrid mode more torque is delivered to the wheels without relevant jerk increase. Moreover, in Fig. 4 is highlighted that during the HEV mode the torque which flows through the clutch is lower then the ICE only mode. This means that the electric motor activation has two advantageous effects, namely reduce both the sliding speed and the transmitted clutch torque. Consequently, less thermal power is generated during the slipping phase in the hybrid mode. This results in a lower clutch material peak temperature as underlined in Fig. 5. Indeed, this graph shows that the temperature rise during the slipping phase is about $32\,^{\circ}\mathrm{C}$ in the ICE only mode and $25\,^{\circ}\mathrm{C}$ in the HEV mode for the given start-up manoeuvre.

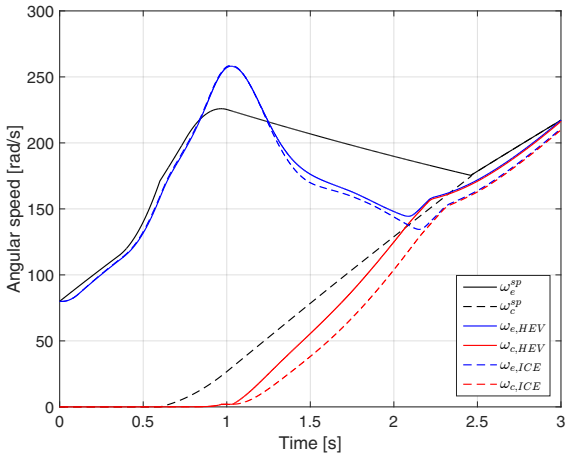

Fig. 3. Angular speeds: HEV mode (blue and red solid lines) and ICE mode (blue and red dashed lines)

Moreover, in Figs. 6 and 7 the requested electric power and the SOC variation are plotted. It is worth noting that the electric motor is activated only for less than $1.5\ s$ thus the used battery capacity is negligible. This is confirmed from the lightly SOC decrease reported in Fig. 7.

In conclusion, the simulation results highlighted that in a single manoeuvre it is possible to reduce the temperature increase of about a quarter with a negligible SOC variation. This means that the electric motor activation can effectively

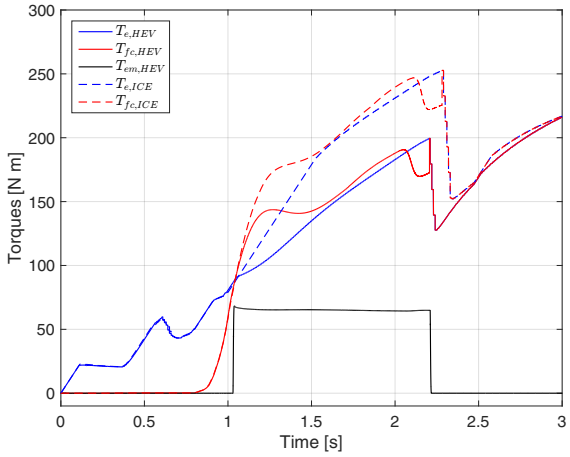

Fig. 4. Torques reduced to primary shaft: HEV mode (solid lines) and ICE mode (dashed lines)

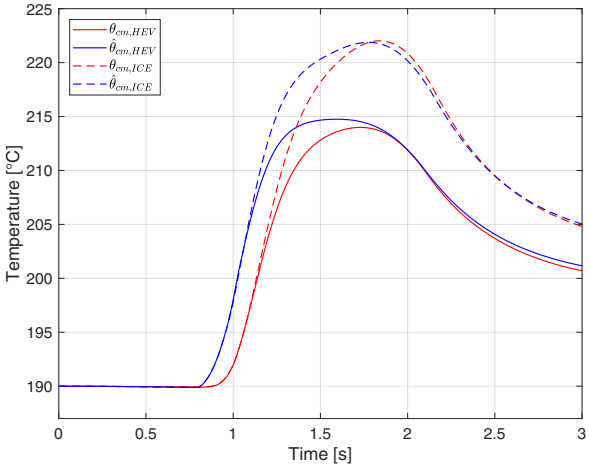

Fig. 5. Interface temperature: HEV mode (blue "estimated" and red "true" solid lines) and ICE mode (blue "estimated" and red "true" dashed lines)

relieve the dry clutch from thermal overheating in heavy working conditions.

VII. CONCLUSION

The goal of this research is to investigate about the role of EM in mild-HEV to assist vehicle launch and relieve dry clutch from thermal damage in hybrid vehicles. To this aim the following simulation scenario has been assumed: initial SOC of 0.25, high initial clutch material temperature (i.e. $190\,^{\circ}\mathrm{C}$) and an up-hill conditions (road slope of 5 degree). The results underlined that in the ICE only mode the peak contact temperature is about $32\,^{\circ}\mathrm{C}$ whereas in the hybrid mode the temperature rise is about $25\,^{\circ}\mathrm{C}$. Furthermore, the used battery capacity and consequently the SOC variation is negligible. Under this light, the electric motor can effectively assist the vehicle launch manoeuvre without strong detrimental influence on SOC level.

REFERENCES

[1] C. C. Chan, *The State of the Art of Electric, Hybrid, and Fuel Cell Vehicles*, Proceedings of the IEEE, vol. 95, no. 4, pp. 704-718, 2007.

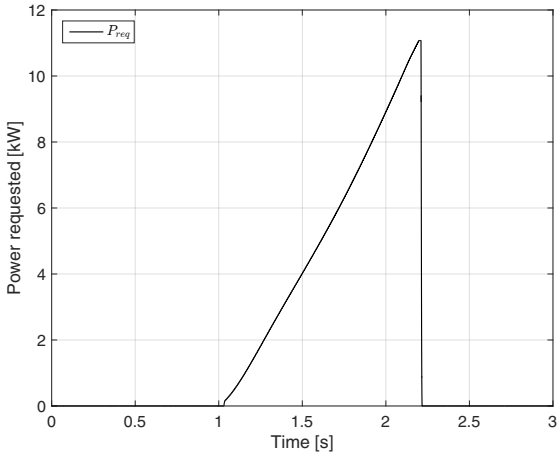

Fig. 6. Requested electric power during the launch maneuvre

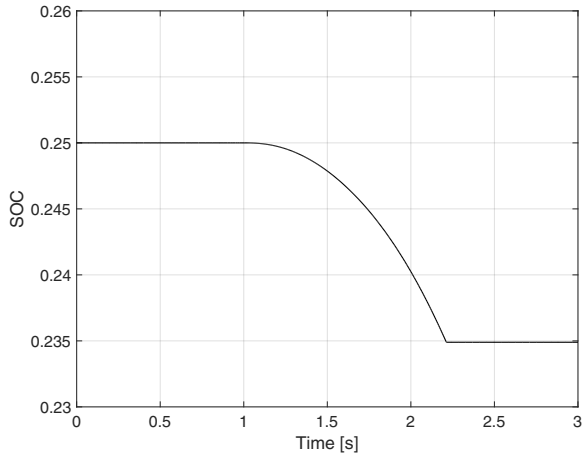

Fig. 7. SOC vs. time

[2] Ali Emadi, *Electric Drive Vehicles*, CRC Press, 2017.

[3] K. T. Chau, *Electric Vehicle Machines and Drives: Design, Analysis and Application*, Wiley-IEEE Press, 2015.

[4] H. Kim and J. Kim and H. Lee, *Mode Transition Control Using Disturbance Compensation for a Parallel Hybrid Electric Vehicle*, Proceedings of the Institution of Mechanical Engineers, Part D: Journal of Automobile Engineering, vol. 225, no. 2, pp. 150-166, 2011.

[5] R. Beck and F. Richert and A. Bollig and D. Abel and S. Saenger and K. Neil and T. Scholt and K. E. Noreikat, *Model Predictive Control of a Parallel Hybrid Vehicle Drivetrain*, Proceedings of the 44th IEEE Conference on Decision and Control, pp. 2670-2675, 2005.

[6] P. D. Walker and N. Zhang, *Active damping of transient vibration in dual clutch transmission equipped powertrains: A comparison of conventional and hybrid electric vehicles*, Mechanism and Machine Theory, vol. 77, pp. 1-12, 2014.

[7] P. Pisu and G. Rizzoni, *A Comparative Study Of Supervisory Control Strategies for Hybrid Electric Vehicles*, IEEE Transactions on Control Systems Technology, vol. 15, no. 3, pp. 506-518, 2007.

[8] K. Oh and J. Min and D. Choi and H. Kim, *Optimization of control strategy for a single-shaft parallel hybrid electric vehicle*, Proceedings of the Institution of Mechanical Engineers, Part D: Journal of Automobile Engineering, vol. 221, no. 5, pp. 555-565, 2007.

[9] L. Guo and B. Gao and Y. Gao and H. Chen, *Optimal Energy Management for HEVs in Eco-Driving Applications Using Bi-Level MPC*, IEEE Transactions on Intelligent Transportation Systems, vol. 18, no. 8, pp. 2153-2162, 2017.

[10] J. Wang and Q. N. Wang and P. Y. Wang and J. N. Wang and N. W. Zou, *Hybrid electric vehicle modeling accuracy verification and global optimal control algorithm research*, International Journal of Automotive Technology, vol. 16, no. 3, pp. 513-524, 2015.

[11] X. Ye, and Z. Jin and X. Hu and Y. Li and Q. Lu, *Modeling and control strategy development of a parallel hybrid electric bus*, International Journal of Automotive Technology, vol. 14, no. 6, pp. 971-985, 2013.

[12] C. Vagg and S. Akehurst and C. J. Brace and L. Ash, *Stochastic Dynamic Programming in the Real-World Control of Hybrid Electric Vehicles*, IEEE Transactions on Control Systems Technology, vol. 24, no. 3, pp. 853-866, 2016.

[13] M. Pisaturo and A. Senatore, *Simulation of engagement control in automotive dry-clutch and temperature field analysis through finite element model*, Applied Thermal Engineering, vol. 93, pp. 958-966, 2016.

[14] G. Pica and C. Cervone and A. Senatore and M. Lupo and F. Vasca, *Dry Dual Clutch Torque Model with Temperature and Slip Speed Effects*, Intelligent Industrial Systems, vol. 2, no. 2, pp. 133-147, 2016.

[15] O. I. Abdullah and J. Schlattmann, *Finite element analysis of temperature field in automotive dry friction clutch*, Tribology in Industry, vol. 34, no. 4, pp. 206-216, 2012.

[16] K. L. Kimming and I. Agner, *Double Clutch: Wet or Dry, this is the question*, LuK Symposium, 2006.

[17] H. Feng and M. Yimin and L. Juncheng, *Study on Heat Fading of Phenolic Resin Friction Material for Micro-automobile Clutch*, Measuring Technology and Mechatronics Automation, 2010 International Conference on, vol. 3, pp. 596-599, 2010.

[18] M. Pisaturo and M. Cirrincione and A. Senatore, *Multiple Constrained MPC Design for Automotive Dry Clutch Engagement*, Mechatronics, IEEE/ASME Transactions on, vol. 20, no. 1, 2015.

[19] M. Pisaturo and M. Cirrincione and A. Senatore, *Influence of the Temperature on the Dry-Clutch Engagement Control in Gear-Shift Manoeuvres*, 23rd Mediterranean Conference on Control & Automation, 2015.

[20] M. Pisaturo and A. Senatore and V. D'Agostino, *Model Predictive Controller for the Clutch Engagement to Limit the Traction Lag due to the Engine Torque Build-up*, The 27th Chinese Control and Decision Conference, pp. 2509-2514, 2015.

[21] C. D. Rakopoulos and E. G. Giakoumis, *Diesel Engine Transiet Operation*, Spinger, 2009.

[22] F. Vasca and L. Iannelli and A. Senatore and G. Reale, *Torque Transmissibility Assessment for Automotive Dry-Clutch Engagement*, Mechatronics, IEEE/ASME Transactions on, vol. 16, no. 3, pp. 564-573, 2011.

[23] V. D'Agostino and M. Pisaturo and A. Senatore, *Improving the Engagement Performance of Automated dry Clutch Through the Analysis of the Influence of the Main Parameters on the Frictional Map*, 5th World Tribology Congress, 2013.

[24] M. Pisaturo and C. D'Auria and A. Senatore, *Friction coefficient influence on the engagement uncertainty in dry-clutch AMT*, 2016 American Control Conference, pp. 7561-7566, 2016.

[25] A. Senatore and C. D'Auria and M. Pisaturo, *Frictional Behaviour and Engagement Control in Dry Clutch Based Automotive Transmissions*, Vehicle Engineering, vol. 4, pp. 1-12, 2017.

[26] V. D'Agostino and N. Cappetti and M. Pisaturo and A. Senatore, *Improving the Engagement Smoothness Through Multi-Variable Frictional Map in Automated Dry Clutch Control*, Proceedings of the ASME2012 International Mechanical Engineering Congress & Exposition, Transportation Systems, vol. 11, 2012.

[27] N. Cappetti and M. Pisaturo and A. Senatore, *Modelling the Cushion Spring Characteristic to Enhance the Automated Dry-Clutch Performance: The Temperature Effect*, Proceedings of the Institution of Mechanical Engineers, Part D: Journal of Automobile Engineering, vol. 226, no. 11, pp. 1472-1482, 2012.

[28] N. Cappetti and M. Pisaturo and A. Senatore, *Cushion spring sensitivity to the temperature rise in automotive dry clutch and effects on the frictional torque characteristic*, Mechanical Testing and Diagnosis, vol. 3, no. 2, pp. 28-38, 2012.

[29] M. Pisaturo and A. Senatore and V. D'Agostino, *Automotive dry-clutch control: Engagement tracking and FE thermal model*, 2016 IEEE 20th Jubilee International Conference on Intelligent Engineering Systems, pp. 69-74, 2016.

[30] M. Pisaturo and A. Senatore and V. D'Agostino, *Could electric motor in HEV assist vehicle launch and relief dry clutch from thermal damage?*, 2017 IEEE International Conference on Advanced Intelligent Mechatronics, pp. 327-333, 2017.

[31] F. Morel and X. Lin-Shi and J. M. Retif and B. Allard and C. Buttay, *A Comparative Study of Predictive Current Control Schemes for a Permanent-Magnet Synchronous Machine Drive*, IEEE Transactions on Industrial Electronics, vol. 56, no. 7, pp. 2715-2728, 2009.

[32] M. Pacas and J. Weber, *Predictive direct torque control for the PM synchronous machine*, IEEE Transactions on Industrial Electronics, vol. 52, no. 2, pp. 1350-1356, 2005.

[33] G. Diana and F. Resta, *Controllo di sistemi meccanici*, Polipress, 2007. "In Italian".

[34] C. Mi and M. A. Masrur and D. W. Gao, *Hybrid Electric Vehicles: Principles and Applications with Practical Perspectives*, Wiley, 2011.

[35] C. Xiang and F. Ding and W. Wang and W. He, *Energy management of a dual-mode power-split hybrid electric vehicle based on velocity prediction and nonlinear model predictive control*, Applied Energy, vol. 189, no. Supplement C, pp. 640-653, 2017.

[36] H. Quanan and S. Jian and L. Lei, *Research on Rapid Testing Platform for TCU of Automated Manual Transmission*, Proceedings of the 2011 Third International Conference on Measuring Technology and Mechatronics Automation - Volume 03, IEEE Computer Society, pp. 67-70, 2011.

[37] M. Sharifzadeh and F. Timpone and A. Farnam and A. Senatore and A. Akbari, *Tyre-Road Adherence Conditions Estimation for Intelligent Vehicle Safety Applications*, Advances in Italian Mechanism Science, pp. 389-398, 2017.

[38] M. Sharifzadeh and A. Akbari and F. Timpone and R. Daryani, *Vehicle tyre/road interaction modeling and identification of its parameters using real-time trust-region methods*, IFAC-PapersOnLine, vol. 49, no. 3, pp. 111-116, 2016.

[39] K. Hebbale and F. Samie and J. Kish, *Dry Dual Clutch Transmission (DCT) Thermal Model*, SAE Technical Paper 2015-01-1144, 2015.

[40] A. Myklebust and L. Eriksson, *Modeling, Observability, and Estimation of Thermal Effects and Aging on Transmitted Torque in a Heavy Duty Truck With a Dry Clutch*, IEEE/ASME Trans. Mechatronics, vol. 20, no. 1, pp. 61-72, Feb. 2015.

[41] J. J. Oh and S. B. Choi, *Real-time estimation of transmitted torque on each clutch for ground vehicles with dual clutch transmission*, IEEE/ASME Trans. Mechatronics, vol. 20, no. 1, pp. 24-36, 2015.

[42] R. Losero and J. Lauber and T-M. Guerra, *Transmitted torque observer applied to real time engine and clutch torque estimation*, IFAC-PapersOnLine, vol. 48, no. 26, pp. 73-78, 2015.

[43] Z. Zhao and L. He and Y. Yang and C. Wu and X. Li and J. Karl Hedrick, *Estimation of torque transmitted by clutch during shifting process for dry dual clutch transmission*, Mechanical Systems and Signal Processing, vol. 75, no. Supplement C, pp. 413-433, 2016.